Synthesis of TiO$_2$(110) ultra-thin films on W(100) and their reactions with H$_2$O

J. Matharu [a], G. Cabailh [a,b], G. Thornton [a,*]

[a] London Centre for Nanotechnology and Chemistry Department, University College London, 20 Gordon Street, London WC1H 0AJ, UK
[b] Institut des Nanosciences de Paris, Université Paris 6 — UPMC and CNRS, 4 Place Jussieu, 75005 Paris, France

ARTICLE INFO

ABSTRACT

We present a study of the growth and reactivity of ultra-thin films of TiO$_2$ grown on W(100). Three approaches to film growth are investigated, each resulting in films that show order in low-energy diffraction (LEED) and a low level of non-stoichiometry in X-ray photoelectron spectroscopy (XPS). H$_2$O is used as a probe of the reactivity of the films, with changes in the Ti 2p and O 1s core levels being monitored by XPS. Evidence for the dissociation of H$_2$O on the TiO$_2$(110) ultra-thin film surface is adduced. These results are discussed with reference to related studies on native TiO$_2$(110).

1. Introduction

Thin films can mimic the surfaces of their bulk counterparts [1] and provide a means to modify stoichiometry in a more controlled fashion. Epitaxial ultra-thin films can be grown on metallic substrates that are well-ordered and exhibit sufficient conducting character to enable study by electron spectroscopy and STM [2–6]. Both of these factors provide a motivation for the current work on TiO$_2$ ultra-thin films. Bennett et al. have previously grown thin films of TiO$_2$ using two deposition methods [7]: Ti deposition on a clean W(100) followed by post-oxidation and Ti deposition on a pre-oxidised W(100) surface. The latter method relies on the formation of a p(2 × 1)-O adlayer following exposure of W(100) to O$_2$ [8,9]. This results in a unit cell of dimensions 6.32 × 3.16 Å^2, which is comparable to the TiO$_2$ (110) unit cell, 6.49 × 2.96 Å^2. The mismatch between these two cells is 2.7% × −6%. In the earlier work, Bennett et al. show that their TiO$_2$ thin films have the rutile structure when using both preparation methods.

Previous structural characterisation work on ultra-thin (<1 nm thickness) films of rutile TiO$_2$(110) is restricted to the use of Ni(110) [10,11], Ni$_{94}$Ti$_6$ (110) [12], Mo(100), (110) and (112) [13–15] and more recently Ag(100) [16] as substrates. Here we look at the extension of the earlier work on thin films on W(100) [7] to the ultra-thin regime, using the reaction with water to provide additional characterisation to LEED and XPS. This complements previous work on ultrathin films on W(100) that examined XPS, UPS and infra-red spectra [17].

Defects in the form of O-vacancies on TiO$_2$(110) are known to be important in the reaction with H$_2$O [18,19]. Hence, one means of investigating the defect character of TiO$_2$(110) ultrathin films is to use H$_2$O as a probe molecule [20]. Surface science studies of the H$_2$O interaction with TiO$_2$(110) surface have built up a picture of the adsorption process and revealed evidence for the presence of surface hydroxyls (as a result of dissociation) at room temperature, accompanied by an increase in Ti^{3+} states [21]. Experiments from Walle et al. suggest that both molecular and dissociative adsorption of H$_2$O occur when a monolayer of water is deposited on a nominally defect free rutile TiO$_2$(110) at 210 K [22]. Only dissociative adsorption of water is observed at room temperature, which involves dissociation at O-vacancies [22,23]. Recent first-principle simulations suggest that water does not dissociate on the defect free surface [24].

Scanning tunnelling microscopy (STM) and non-contact atomic force microscopy (NC-AFM) have provided insight into the mechanism of dissociation [23,25–28]. The currently accepted mechanism is that H$_2$O molecules adsorb at O vacancy sites (O$_{vac}$) and dissociate, resulting in a pair of hydroxyls in the bridging row (OH$_b$): one in place of the original O$_{vac}$, and a second formed from the dissociated H atom and another bridging row oxygen atom (O$_b$). The resulting OH$_b$ pair and its related charges play an important role in reactivity of the surface with O$_2$ [28]. Here we examine the morphology of TiO$_2$(110) ultra-thin films, their electronic structure as well as their reactivity with H$_2$O.

2. Experimental

Experiments were conducted in an ultra high vacuum (UHV) chamber with a base pressure of 3 × 10^{-10} mbar. Data were recorded at room

* Corresponding author. Tel.: +44 2076797979.
E-mail addresses: matharujai@gmail.com (J. Matharu), cabailh@insp.upmc.fr (G. Cabailh), g.thornton@ucl.ac.uk (G. Thornton).

temperature, using an unpolarised Mg Kα radiation source ($h\nu =$ 1253.6 eV) and a *VSW/Omicron* EA125 hemispherical analyser. The angle of incidence of X-ray photons was 67.5° with respect to the surface normal, with photoelectrons collected at normal emission. A pass-energy of 40 eV was used, giving an energy resolution (full width at half maximum) of 0.3 eV. Binding energies are measured relative to the Fermi level, which was recorded from the Ta sample holder.

The W(100) crystal (Surface Preparation Laboratory) was cleaned by Ar$^+$ sputtering, followed by repeated cycles of annealing in 1×10^{-7} mbar of high purity O$_2$ (SIP Analytical, 99.5%) at 1100 K and flash annealing in UHV to 2000 K to remove the principal contaminants (O and C) [29]. The clean surface was characterised by a sharp (1×1) LEED pattern and the absence of O 1s and C 1s peaks in XPS spectra.

Ti was deposited using a home-built electron beam evaporator. The doser was calibrated using the intensity ratios of the Ti 2p, W 4p and W 4d XPS peaks. Breakpoints in the ratios indicate monolayer coverage [30] and can be used to monitor the amount of Ti deposited. Oxidation of deposited Ti was achieved by annealing in 1×10^{-7} mbar O$_2$ at 800 K for 2 h. Films were characterised by a TiO$_2$(110) (1×1) LEED pattern with additional spots along the principal azimuths [7]. Film thicknesses were estimated from the areas of the Ti 2p and W 4d XPS peaks using the method described by Susaki et al. [31], correcting the peak areas to account for ionisation cross sections and for the analyser transmission function. One monolayer equivalent (MLE) is defined as the number of TiO$_2$ surface unit cells that will uniformly cover the surface of the W(100) substrate. De-ionised H$_2$O was degassed using freeze-pump-thaw cycles. The sample was exposed to H$_2$O as well as O$_2$ by backfilling the chamber to a pressure of 1×10^{-7} mbar.

3. Results

3.1. TiO$_2$ thin film growth

Three approaches to ultra-thin film growth were used, the first two being similar to those employed by McCavish et al. who have studied a coverage regime from 5 to 30 monolayers [7]. In one approach, Ti was deposited in UHV onto a clean W(100) surface (two-stage growth). The second method consisted of depositing Ti in UHV onto a pre-oxidised W(100) surface (pre-oxidised growth) and the third depositing Ti in a partial pressure of O$_2$ (reactive growth). All these depositions were followed by post-oxidation in O$_2$. Ti deposited on the clean W surface is metallic in nature. This is evident from XPS of the Ti 2p region, showing asymmetric Doniach–Sunjic type peaks [32] at $E_B = 454.7$ eV ($2p_{3/2}$) and 460.7 eV ($2p_{1/2}$) (1.6 MLE film, Fig. 1(a)) [33]. After annealing in 1×10^{-7} mbar O$_2$ at 800 K for 2 h, oxidation causes the Ti 2p core levels to shift to 459.0 eV ($2p_{3/2}$) and 464.7 eV ($2p_{1/2}$), typical of Ti^{4+} [34,35] (Fig. 1(a)).

In the case of pre-oxidised growth, where Ti is deposited on the W surface previously annealed in 1×10^{-7} mbar O$_2$ at 800 K for 3 min, the Ti 2p XPS peaks are broader than for Ti deposited on the clean W surface (1.2 MLE film, Fig. 1(b)). This broadening can be assigned to the presence of oxidised species of Ti (i.e. Ti^{2+} and Ti^{3+}). The main peaks of these species are positioned at $E_B = 457.1$ eV (Ti^{3+}) and 455.4 eV (Ti^{2+}). As for the case of the two-stage growth, these peaks shift to positions associated with Ti^{4+} states after a 2 h anneal in O$_2$.

Depositing Ti in a background pressure of 1×10^{-7} mbar O$_2$ initially results in a Ti 2p XPS spectrum showing contributions from Ti^{4+} states as well as reduced Ti^{3+} and Ti^{2+} states, indicating incomplete oxidation [34] as shown for a 1.2 MLE film (Fig. 1(c)). After a 2 h anneal in O$_2$, the Ti 2p core level width decreases as Ti^{2+} states (at $E_B = 455.4$ eV and 460.8 eV) are completely removed. By contrast the Ti^{3+} states are not completely removed, indicating that the film is slightly substoichiometric.

TiO$_2$(110) films between 0.2 and 5.7 MLE thick were synthesised. In all cases, on deposition of Ti the observed LEED pattern has a very high
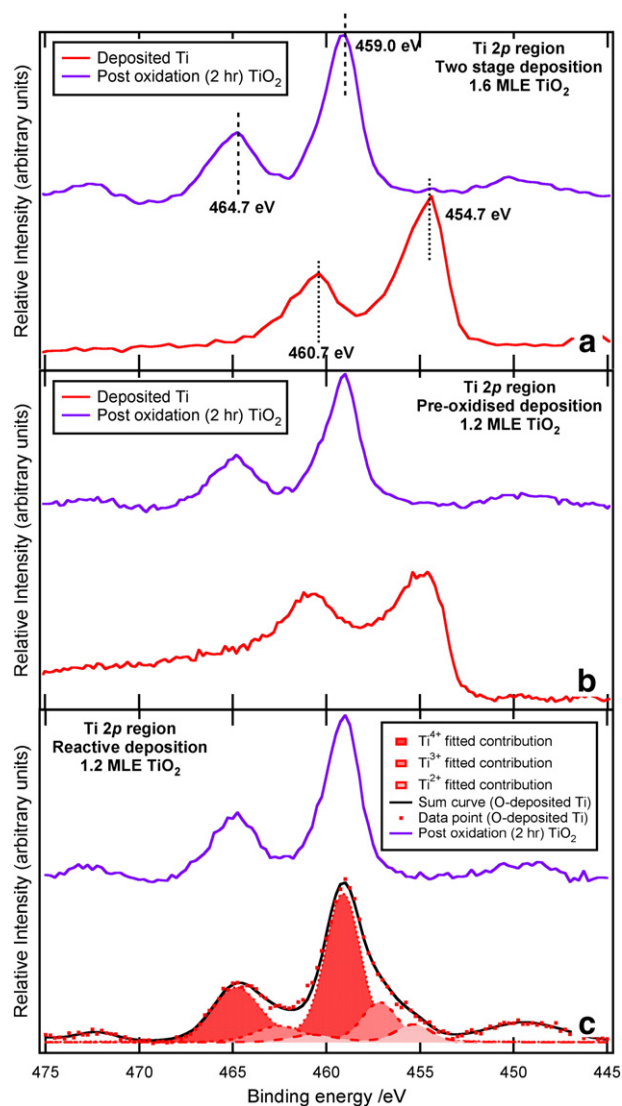
Fig. 1. MgKα XPS spectra ($h\nu = 1253.6$ eV) of W(100) showing (a) the shift in E$_B$ of the Ti 2p core levels after oxidation in 1×10^{-7} mbar O$_2$ for 2 h at 800 K for the two stage growth, (b) the broadened Ti 2p core levels of Ti deposited on an oxidised W(100) surface (bottom) and the shift to fully oxidised peaks after oxidation in 1×10^{-7} mbar O$_2$ for 2 h at 800 K (top) and (c) the mixed valence Ti states on depositing Ti in 1×10^{-7} mbar O$_2$ (bottom), and the removal of these states on oxidation in 1×10^{-7} mbar O$_2$ for 2 h at 800 K (top, blue). Spectra are normalised to the same maximum intensity and Shirley backgrounds have been subtracted. The peak at 449 eV corresponds to the Ti 2p satellites from Mg Kα$_{3,4}$ excitation. Ti 2p spectra were fitted with three doublets (Voigt functions) corresponding to the Ti^{2+} (light red), Ti^{3+} (red) and Ti^{4+} (dark red) contributions, as shown for the reactive deposition method (c). The sum of the fitted contributions is represented by the black line and the experimental data by red dots. A polynomial plus Shirley background was subtracted. The peak widths, branching ratio, and spin-orbit-splitting were kept constant throughout and are summarised in Table 1.

background with faint (1×1) spots from the W(100) substrate. This indicates the absence of long range order associated with the deposited Ti using the three different growth methods. Following annealing in O$_2$, oxidised films produce LEED patterns (Fig. 2(c)) that are a composite of the (1×1) spots from the W(100) substrate (Fig. 2(a)) and the (1×1) spots from an ordered TiO$_2$(110) surface (Fig. 2(b)). For films of thickness <1 MLE, the LEED beams are faint, likely due to incomplete coverage of the W(100) substrate and oxidation of regions of bare W. For films as thick as 5.7 MLE, the substrate diffraction spots are still visible, indicating that the thin films do not entirely cover the substrate surface.
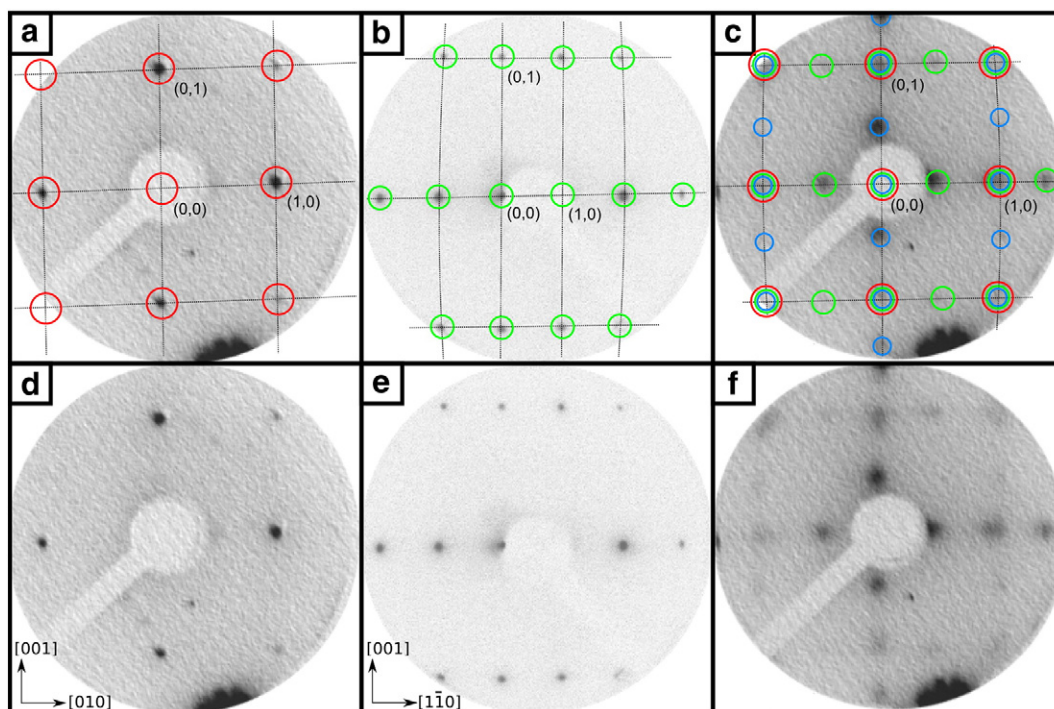
Fig. 2. LEED patterns for (a) the clean W(100) surface (beam energy, E_{beam} = 55 eV), with red circles indicating (1 × 1) spots; (b) a reference TiO_2(110) crystal (E_{beam} = 66 eV), with the green circles indicating TiO_2(110) (1 × 1) spots and (c) a 5.8 MLE TiO_2 film grown by the pre-oxidised method on W(100) (E_{beam} = 55 eV). The green and blue circles indicate the two TiO_2 domains. The figures are reproduced (d–f) without the symbols for clarity. The azimuthal orientations of the single crystals are indicated.

The final pattern is a two-domain (2 × 1) with respect to the initial W(100) pattern, with two TiO_2 domains rotated 90° and aligned with the main directions of the substrate, as observed in the earlier work [7].

Examination of Ti 2p XPS spectra shows that films synthesised using the pre-oxidised method are not completely stoichiometric and that contributions from both Ti^{3+} and Ti^{4+} states are present (Fig. 3). Using the fitting parameters in Table 1, we use the Ti 2p spectrum to estimate the % Ti^{3+} states (Table 2). Non-stoichiometry may arise due to strain in the films resulting from the lattice mismatch and from surface defects. A correlation between thickness and non-stoichiometry has been previously observed [7] with non-stoichiometry decreasing with increased thickness. Curve fitting of the corresponding O 1s XPS spectra reveals two contributions (Fig. 3), one centred around a binding energy of 530.4 eV that corresponds to oxygen in the selvedge, and a satellite peak, denoted S_1 shifted + 1.4 eV from the main peak (fitting parameters shown in Table 1). S_1 was assigned to two-fold bridging oxygen atoms (O_b) on the TiO_2 surface in earlier work [36–38]. However, more recent studies have instead suggested that this peak is due to OH_b arising from reaction with residual water in the background vacuum [11,39]. The S_1 contribution, expressed as a percentage of the total O 1s peak area, is greater in films <1 MLE TiO_2 thick.

The nature of the substrate–film interface can be investigated by comparison of the W 4d XPS spectra for different stages of the growth process [7]. Upon adsorption of oxygen there is a slight broadening of the W 4d XPS peaks at higher binding energy compared with the clean surface (Fig. 4(a)). Streaking along the principal azimuths is also observed in the LEED pattern and with sufficient exposure to oxygen this sharpens to a (4 × 1) pattern as observed in [40]. There is no apparent change between the W 4d XPS spectra of the clean W surface and a Ti-deposited W surface (Fig. 4(b)). This is also the case between the W 4d spectrum of a fully oxidised TiO_2 film and the oxidised W surface (Fig. 4(c)).

### 3.2. Interaction with H_2O

As a preliminary measurement, a clean W(100) surface was exposed to up to 100 l H_2O (1 L = 1.32 × 10^{-6} mbar s^{-1}). There has been a previous study of H_2O adsorption on W(100), which employed synchrotron radiation photoemission [41]. This indicated dissociative adsorption with formation of W–O bonds. Fig. 5(a) shows the changes in O 1s XPS spectra as H_2O exposure increases. Even with very thorough cleaning, a trace amount of oxygen is present on the nominally clean surface. The intensity of this peak increases on exposure to H_2O and it can be fitted with two Gaussian–Lorentzian singlet peaks at 530.5 eV and 532.9 eV. Using the area of these peaks and the area of the W 4d XPS spectra, the atomic concentration ratio of O and W is seen to increase exponentially (Fig. 5(b)) to a saturation limit of 0.15 and 0.05 for the peaks at 530.5 eV and 532.9 eV, respectively. The peak at 530.5 eV corresponds to what is expected for adsorbed atomic oxygen [42]. An E_B of 532.9 eV corresponds to that expected for molecular water [41].

TiO_2 thin films prepared by the pre-oxidised W(100) method were exposed to ≤200 L H_2O in stages at 293 K. No change was observed in the LEED pattern, aside from attenuation of spots indicating adsorption without long range order. Changes to the stoichiometry of films upon H_2O exposure were monitored through the evolution of the Ti 2p XPS spectra. These are shown for two of the films, with thicknesses of 0.9 MLE TiO_2 (Fig. 6(a–c)) and 5.3 MLE TiO_2 (Fig. 7(a–c)). In both cases, there is an increase in the Ti^{3+} concentration.

For the thinnest film, increases on the lower E_B side of the Ti 2p doublet are apparent upon water exposure (see Fig. 6(a)). The difference spectrum for each exposure shows a doublet at 458.1 eV and 463.5 eV up to 187 L H_2O exposure, which evidences the presence of Ti^{3+} states (Fig. 6(b)). For large exposure, the doublet peak in the difference spectra gains some asymmetry to lower E_B. This can be fitted with another
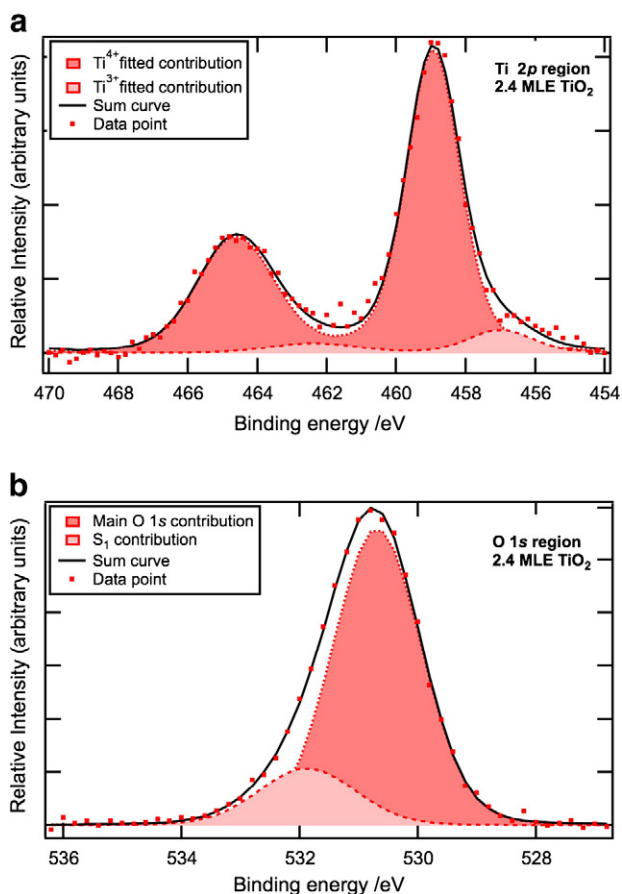
Fig. 3. MgKα XPS spectra (hv = 1253.6 eV) after Shirley background subtraction of a 2.4 MLE thick TiO$_2$ film grown using the pre-oxidised W(100) method. (a) Ti 2p region showing contributions from Ti^{3+} and Ti^{4+} ions, as estimated by fitting with two Gaussian–Lorentzian doublets. Ti^{3+} ions make up 9% of the overall Ti contribution. (b) O 1s region showing contributions from the main O 1s XPS peak and the S$_1$ satellite. The latter accounts for 27% of the total O 1s XPS peak area.

Table 2

Summary of initial values for %Ti^{3+} and %S$_1$ for TiO$_2$(110) ultra-thin films on W(100) of varying thickness prepared by the pre-oxidised method. The corresponding figures are given for the spectra following a saturation exposure to water at 1×10^{-8} mbar.

TiO$_2$ thickness /MLE	Initial %Ti^{3+}	Initial % S$_1$	Saturation % Ti^{3+}	Saturation % S$_1$
0.9	5.0 ± 2.4	26.3 ± 1.2	37.2 ± 3.1	35.0 ± 1.8
1.6	6.6 ± 2.1	27.0 ± 1.3	15.3 ± 1.2	29.4 ± 1.0
4.2	4.5 ± 2.4	29.7 ± 1.4	15.3 ± 1.1	32.6 ± 1.1
5.3	0.0 ± 1.0	24.0 ± 2.7	17.5 ± 2.8	31.1 ± 1.4

peaks at 458.1 eV and 463.5 eV, corresponding to Ti^{3+} features (Fig. 7(b)). The increase in %Ti^{3+} features reaches a maximum of 18% at 60 L for the 5.3 MLE film.

doublet at 455.4 eV and 460.8 eV and suggests the presence of Ti^{2+} states [34]. By peak fitting and comparing peak areas, the relative concentration of Ti^{3+} and Ti^{2+} can be estimated (Fig. 8). Plotting these values against exposure (Fig. 6(c)) shows an increase in %Ti^{3+}, nearing a maximum at 37% Ti^{3+} after 100 L exposure. A shallower increase to a maximum of 20% Ti^{2+} is observed, with Ti^{2+} features not present below 7 L exposure. In thicker films, no Ti^{2+} features are observed. However, an increase in Ti^{3+} concentration is still observed in the Ti 2p spectra (Fig. 7(a)). The doublet peak appearing in difference spectra is more symmetric and can be fitted with a single doublet with XPS

Table 1

Parameters used in Ti 2p (Figs. 1, 3 and 8) and O 1s (Fig. 3) fitting procedures, showing peak position and Gaussian–Lorentzian (Voigt function) full-width at half-maximum (FWHM) values.
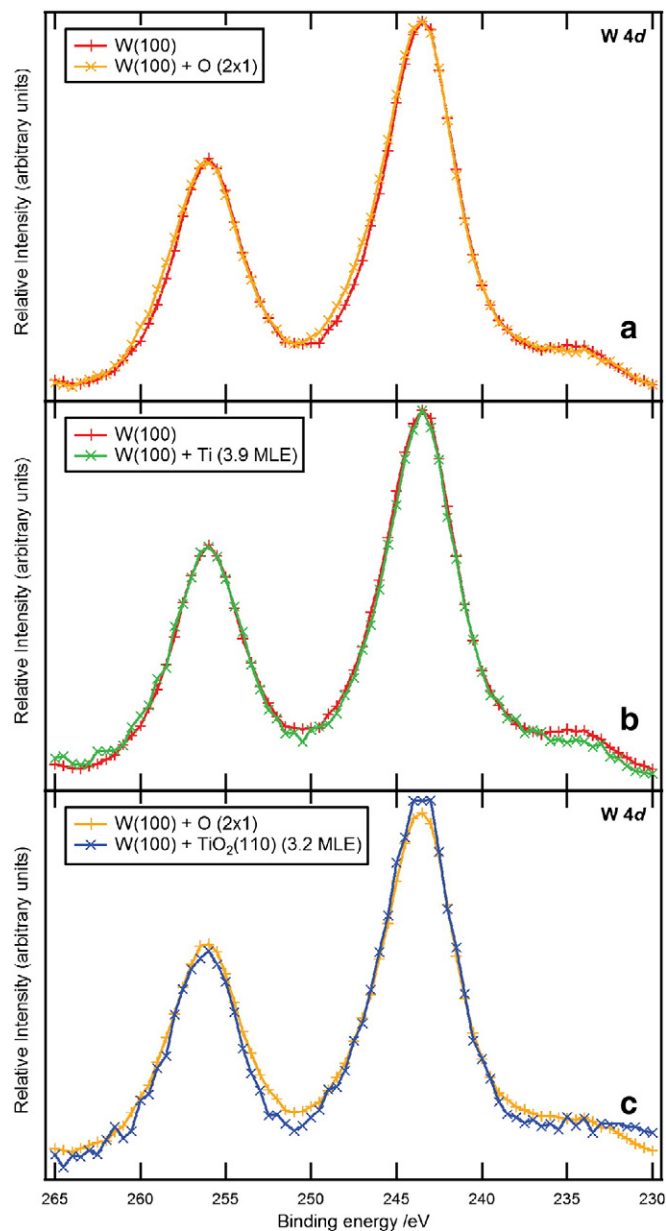
		Position/eV	FWHM/eV
Ti^{4+}	2$p_{3/2}$	459.0	2.16
	2$p_{1/2}$	464.8	2.97
Ti^{3+}	2$p_{3/2}$	457.1	2.20
	2$p_{1/2}$	462.5	2.99
Ti^{2+}	2$p_{3/2}$	455.4	2.22
	2$p_{1/2}$	460.8	3.02
O 1s		530.4	1.82
S$_1$		531.8	2.06

Fig. 4. Comparison of the MgKα W 4d XPS spectra (hv = 1253.6 eV) for (a) W(100) and W(100)-(2 × 1)-O surfaces, (b) W(100) and Ti-deposited (3.9 MLE Ti) W(100) surfaces, and (c) W(100)-(2 × 1)-O surface and a fully oxidised TiO$_2$(110) thin film on W(100) (grown using the two-stage method). Shirley backgrounds have been subtracted and spectra are normalised to the same maximum intensity.
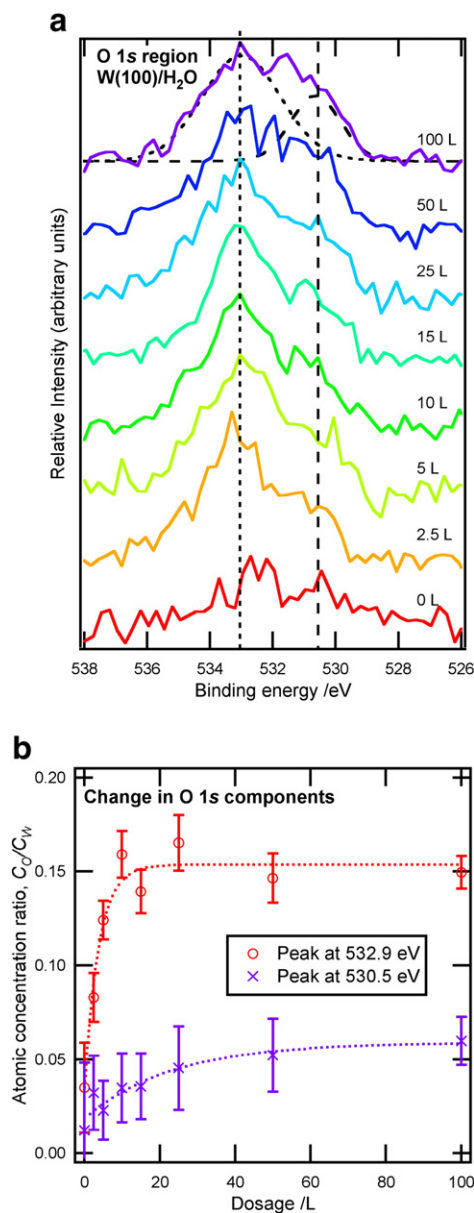
Fig. 5. (a) MgKα XPS spectra ($h\nu = 1253.6$ eV) of the O 1s region for W(100) exposed to H_2O at 300 K. Shirley backgrounds have been subtracted. (b) Atomic concentration ratio C_O/C_W as a function of exposure to H_2O, where C_O and C_W correspond to the peak areas of O 1s and W 4d, respectively. The ratio in atomic concentration increases exponentially to a saturation limit of 0.15 and 0.05 for the peaks at 532.9 eV (red) and 530.5 eV (blue), respectively.

Changes in the O 1s XPS spectra are shown for the same two films: 0.9 MLE TiO_2 (Fig. 6(d–f)) and 5.3 MLE (Fig. 7(d–f)). An increase at higher E_B is observed upon increasing H_2O exposure (Figs. 6(d), 7(d)). This increase is more apparent in the difference spectra of each scan after subtraction of the 0 L H_2O exposure spectrum (Figs. 6(e), 7(e)). Peak fitting of the difference spectra reveal an increase in a feature at an E_B of 531.8 eV, corresponding to the position of the S_1 satellite referred to above. This increases to a maximum value of 35% of the total O 1s area for the 0.9 MLE film and 31% for the 5.3 MLE film. The higher increase for the thinner film can be related to the higher increase in Ti^{3+} states which are twice as large for the 0.9 MLE film (~32%) compared to the thicker films (~16%). For the 0.9 MLE film, an increase is also seen in

a feature at an E_B of 533.0 eV denoted S_2. Initial and saturation values of %Ti^{3+} and %S_1 for the films are tabulated in Table 2.

4. Discussion

LEED data indicate that there is no long-range order associated with Ti deposited on W surfaces, but that ordered TiO_2(110) films result post-oxidation. The LEED patterns are sharper for thicker films presumably because the TiO_2 islands are larger and the strain due to the lattice mismatch between the substrate and the film decreases with increasing thickness. The similarity in the Ti 2p and O 1s XPS spectra for each of the growth methods used suggests that films produced by each route are more or less equivalent. At the temperature at which the films are annealed (800 K), oxygen can diffuse through TiO_2 [43] and films can be completely oxidised regardless of initial conditions. Strain, as well as surface defects such as O_{vac} can also explain the slight non-stoichiometry. The W 4d spectrum of the W/TiO_2 interface is similar to the same spectrum for oxidised W, suggesting that the film layer at the substrate interface consists of O atoms rather than Ti.

The increase in Ti^{3+} states on exposure to H_2O suggests dissociation on the TiO_2 thin film surface, with resulting charge transfer from hydroxyl species to Ti^{4+} [21]. The O 1s XPS data is consistent with this picture, showing an increase in intensity of the OH peak (S_1), with no increase of a feature at the position expected for molecular H_2O (2.5 to 3.5 eV higher BE). For the 0.9 MLE film the increase in height of S_2 will arise from molecular adsorption on bare areas of W(100)-O. The values of %Ti^{3+} increase with H_2O exposure for all films (Table 2), whereas Ti^{2+} states are only detected for the exposure of the 0.9 MLE TiO_2 thick film to H_2O. Since the film is of <1 MLE thickness, the W(100)-O surface is not completely covered with TiO_2 and the formation of lower oxides such as TiO is possible, especially at island edges. The asymmetry of the O 1s difference spectra upon H_2O exposure for the 0.9 MLE film can also be explained by exposure of the W(100)-O surface to water (Fig. 6e). Changes in the S_1 contribution (531.8 eV) as well as the feature arising from H_2O adsorption on exposed W (532.9 eV), where H_2O oxidises the W surface to WO_3 and WO_{3-x} [42] will contribute intensity to the difference spectra.

In the experiments presented here, the %S_1 increases exponentially to a maximum saturation value and is assigned to the presence of adsorbed hydroxyls. The presence of S_1 prior to H_2O exposure will be due to dissociative adsorption of H_2O from the residual vacuum [11].

5. Conclusions

Three methods of synthesising ultra-thin films of TiO_2(110) on a W(100) substrate have been investigated using XPS and LEED. The resulting films have been found to be equivalent, with films between 0.2 and 5.7 MLE being synthesised. The reactivity of the TiO_2(110) surface has been examined by exposing to H_2O. An increase in adsorbed hydroxyls, OH_b, accompanies an increase in Ti^{3+} states, consistent with an increase in excess charge on the TiO_2(110) surface. Molecular H_2O was not observed spectroscopically except for films of <1 MLE TiO_2 thickness, where regions of exposed WO_x are present and can be hydrated, as shown by exposure of a clean W surface to H_2O. The findings of this study are in line with experiments previously reported in the literature using native surfaces of TiO_2 and on ultra-thin films of TiO_2(110) [10–16]. We note that ultra-thin TiO_2 films grown on W(100) would be suitable for use in electron spin resonance experiments, since the substrate is paramagnetic.
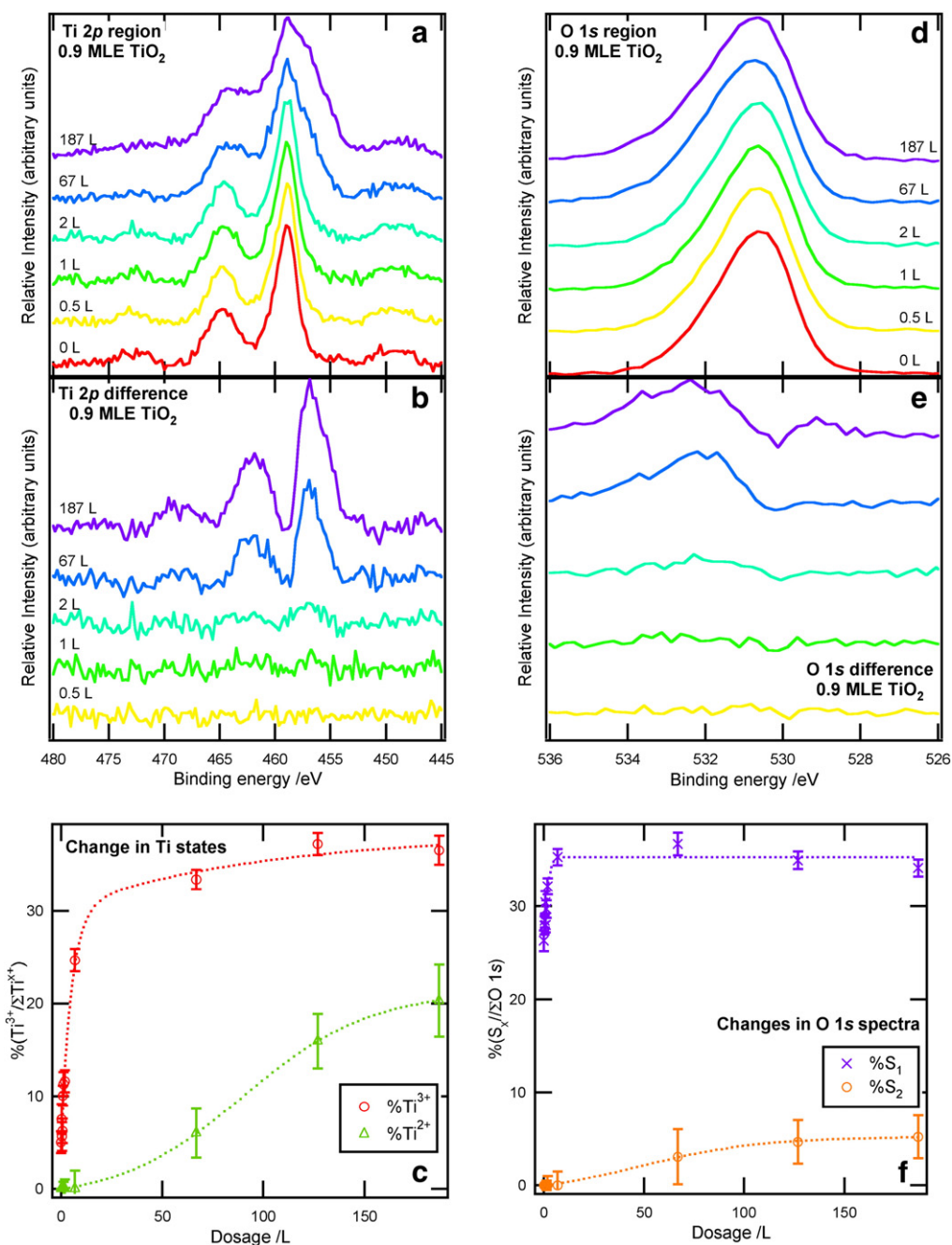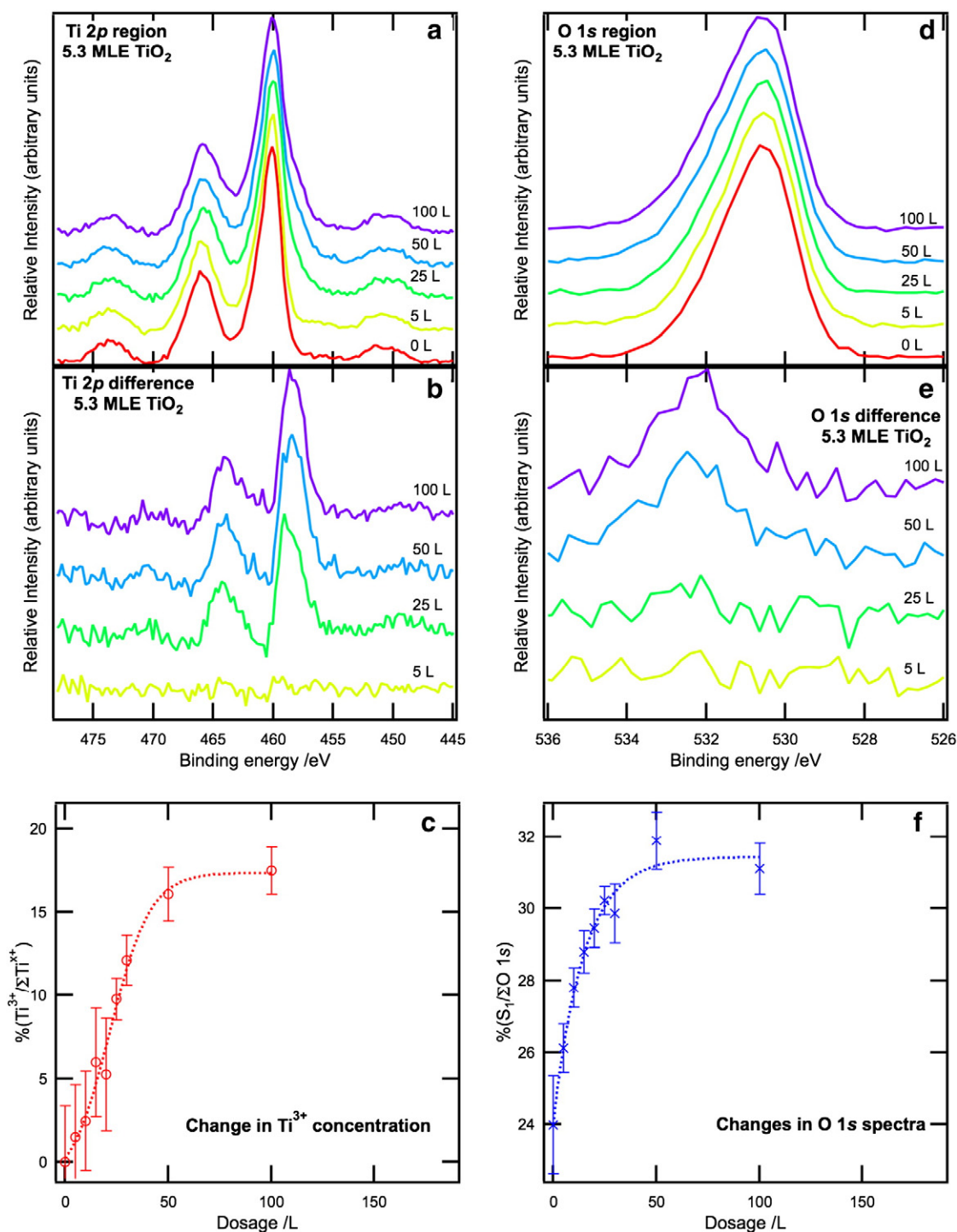
Fig. 6. MgKα XPS spectra ($h\upsilon = 1253.6$ eV) of W(100) after growth of a 0.9 MLE TiO_2 thin film (pre-oxidised growth). The spectra are presented as a function of H_2O exposure up to 187 L at 300 K: (a) Ti 2p region spectra at each exposure, (b) difference spectra showing changes compared with the film prior to H_2O exposure, (c) change in %Ti^{3+} upon H_2O exposure, (d) O 1s region spectra as a function of exposure; (e) difference spectra showing changes compared with the film prior to H_2O exposure; (f) change in %S_1 and %S_2 of the O 1s signal upon H_2O exposure.

References

[1] S.A. Chambers, Surf. Sci. Rep. 39 (2000) 105.
[2] C.R. Henry, Surf. Sci. Rep. 31 (1998) 231.
[3] R.M. Jaeger, H. Kuhlenbeck, H.-J. Freund, M. Wuttig, W. Hoffmann, R. Franchy, H. Ibach, Surf. Sci. 259 (1991) 235.
[4] G.S. Herman, M.C. Gallagher, S.A. Joyce, C.H.F. Peden, J. Vac. Sci. Technol. B 14 (1996) 1126.
[5] D.C. Grinter, R. Ithnin, C.L. Pang, G. Thornton, J. Phys. Chem. C 114 (2010) 17036.
[6] S.C. Street, C. Xu, D.W. Goodman, Annu. Rev. Phys. Chem. 48 (1997) 43.
[7] N.D. McCavish, R.A. Bennett, Surf. Sci. 546 (2003) 47.
[8] H. Yamazaki, T. Kamisawa, T. Kokubun, T. Haga, S. Kamimizu, K. Sakamoto, Surf. Sci. 477 (2001) 174.
[9] H. Yamazaki, S. Kamimizu, K. Hara, K. Sakamoto, Surf. Sci. 538 (2003) L505.
[10] T.V. Ashworth, G. Thornton, Thin Solid Films 400 (2001) 43.
[11] A.C. Papageorgiou, G. Cabailh, Q. Chen, A. Resta, E. Lundgren, J.N. Andersen, G. Thornton, J. Phys. Chem. C 111 (2007) 7704.
[12] A. Atrei, U. Bardi, G. Rovida, Surf. Sci. 391 (1997) 216.
[13] W.S. Oh, C. Xu, D.Y. Kim, D.W. Goodman, J. Vac. Sci. Technol. A 15 (1997) 1710.
[14] X. Lai, Q. Guo, B.K. Min, D.W. Goodman, Surf. Sci. 487 (2001) 1.
[15] D. Kumar, M.S. Chen, D.W. Goodman, Thin Solid Films 515 (2006) 1475.
[16] A. Atrei, B. Cortigiani, A.M. Ferrari, J. Phys. Condens. Matter 24 (2012) 445005.
[17] R.A. Bennett, J.S. Mulley, M.A. Newton, M. Surman, J. Chem. Phys. 127 (2007) 084707.
[18] M.A. Henderson, Surf. Sci. 355 (1996) 151.
[19] M.A. Henderson, Langmuir 12 (1996) 5093.
[20] C.L. Pang, R. Lindsay, G. Thornton, Chem. Soc. Rev. 37 (2008) 2328.
[21] R.L. Kurtz, R. Stockbauer, T.E. Madey, E. Román, J.L. de Segovia, Surf. Sci. 218 (1989) 178.

Fig. 7. MgKα XPS spectra ($h\nu = 1253.6$ eV) of W(100) after growth of a 5.3 MLE TiO$_2$(110) thin film (pre-oxidised growth). The spectra are presented as a function of H$_2$O exposure up to 100 L at 300 K: (a) Ti 2p region at each exposure; (b) difference spectra showing changes compared with the film prior to H$_2$O exposure; (c) change in %Ti^{3+} upon H$_2$O exposure; (d) O 1s region at each exposure; (e) difference spectra showing changes compared with the film prior to H$_2$O exposure; (f) change in %S$_1$ O 1s signal upon H$_2$O exposure. All spectra have had a Shirley background removed.

[22] L.E. Walle, A. Borg, P. Uvdal, A. Sandell, Phys. Rev. B 80 (2009) 235436.
[23] S. Wendt, R. Schaub, J. Matthiesen, E.K. Vestergaard, E. Wahlström, M.D. Rasmussen, P. Thostrup, L.M. Molina, E. Lægsgaard, I. Stensgaard, B. Hammer, F. Besenbacher, Surf. Sci. 598 (2005) 226.
[24] L.-M. Liu, C. Zhang, G. Thornton, A. Michaelides, Phys. Rev. B 82 (2010) 161415R.
[25] I.M. Brookes, C.A. Muryn, G. Thornton, Phys. Rev. Lett. 87 (2001) 266103.
[26] O. Bikondoa, C.L. Pang, R. Ithnin, C.A. Muryn, H. Onishi, G. Thornton, Nat. Mater. 5 (2006) 189.
[27] Z. Zhang, O. Bondarchuk, B.D. Kay, J.M. White, Z. Dohnálek, J. Phys. Chem. B 110 (2006) 21840.

[28] A.C. Papageorgiou, N.S. Beglitis, C.L. Pang, G. Teobaldi, G. Cabailh, Q. Chen, A.J. Fisher, W.A. Hofer, G. Thornton, Proc. Natl. Acad. Sci. 107 (2010) 2391.
[29] M. Grunze, H. Ruppender, O. Elshazly, J. Vac. Sci. Technol. A 6 (1988) 1266.
[30] I. Vaquila, M.C.G. Passeggi Jr., J. Ferrón, Phys. Rev. B 55 (1997) 13925.
[31] T. Susaki, T. Komeda, M. Kawai, Phys. Rev. Lett. 88 (2002) 187602.
[32] S. Doniach, M. Šunjić, J. Phys. C Solid State Phys. 3 (1970) 285.
[33] In: A.C. Thompson, D. Vaughan (Eds.), X-Ray Data Booklet, 2nd edition, Lawrence Berkeley National Laboratory, University of California, 2001, (http://xdb.lbl.gov/xdb.pdf).
[34] B. Siemensmeyer, J.W. Schultze, Surf. Interface Anal. 16 (1990) 309.
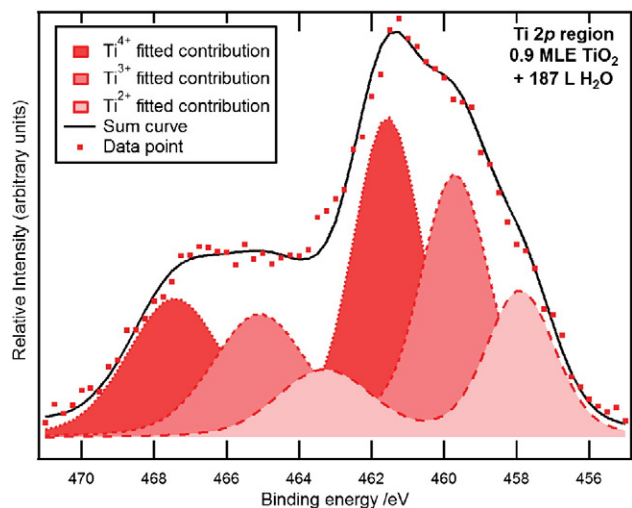
Fig. 8. MgKα XPS spectrum ($h\nu = 1253.6$ eV) of a 0.9 MLE TiO$_2$(110) film (pre-oxidised growth) on W(100) after exposure to 187 L H$_2$O at 300 K. The spectrum has been Shirley background subtracted. Contributions from Ti^{2+}, Ti^{3+} and Ti^{4+} ions are highlighted. They were estimated by fitting with three Gaussian–Lorentzian doublets. The concentrations of Ti^{2+} and Ti^{3+} are 20% and 37%, respectively.

[35] C.N. Sayers, N.R. Armstrong, Surf. Sci. 77 (1978) 301.
[36] T.K. Sham, M.S. Lazarus, Chem. Phys. Lett. 68 (1979) 426.
[37] E.L. Bullock, L. Patthey, S.G. Steinemann, Surf. Sci. 352–354 (1996) 504.
[38] J. Cardenas, S. Sjöberg, Surf. Sci. 532–535 (2003) 1104.
[39] L.-Q. Wang, D.R. Baer, M.H. Engelhard, A.N. Shultz, Surf. Sci. 344 (1995) 237.
[40] E. Bauer, H. Poppa, Y. Viswanath, Surf. Sci. 58 (1976) 517.
[41] D. Mueller, A. Shih, E. Roman, T. Madey, R. Kutz, R. Stockbauer, J. Vac. Sci. Technol. A 6 (1988) 1067.
[42] In: E. Lassner, W.-D. Schubert (Eds.), Tungsten: Properties, Chemistry, Technology of the Element, Alloys and Chemical Compounds, Springer, New York, 1999.
[43] J.T. Mayer, U. Diebold, T.E. Madey, E. Garfunkel, J. Electron Spectrosc. Relat. Phenom. 73 (1995) 1.